Probing the Atmospheric Cl Isotopic Ratio on Mars: Implications for Planetary Evolution and Atmospheric Chemistry

G. Liuzzi[1,2*], G. L. Villanueva[1], S. Viscardy[3], D. Mège[4], M. M. J. Crismani[5], S. Aoki[3,6], J. Gurgurewicz[4], P.-A. Tesson[4], M. J. Mumma[1], M. D. Smith[1], S. Faggi[1,2], V. Kofman[1,2], E. Knutsen[1,2], F. Daerden[3], L. Neary[3], F. Schmidt[7], L. Trompet[3], J. T. Erwin[3], S. Robert[3,8], I. R. Thomas[3], B. Ristic[3], G. Bellucci[9], J. J. Lopez-Moreno[10], M. R. Patel[11,12], A. C. Vandaele[3]

[1] NASA Goddard Space Flight Center, 8800 Greenbelt Rd., Greenbelt, 20771 MD, USA
[2] Dept. of Physics, American University, 4400 Massachusetts Av., Washington, 20016 DC, USA
[3] Royal Belgian Institute for Space Aeronomy, BIRA-IASB, 3 Avenue Circulaire, 1180 Brussels, Belgium
[4] Centrum Badań Kosmicznych Polskiej Akademii Nauk (CBK PAN), Bartycka 18A, 00-716 Warszawa, Poland
[5] California State University San Bernardino, 5500 University Pkwy, San Bernardino, CA 92407
[6] LPAP, STAR Institute, Université de Liège, Allée du 6 août, 19C, 4000 Liège, Belgium
[7] Université Paris-Saclay, CNRS, GEOPS, 91405, Orsay, France
[8] Institute of Condensed Matter and Nanosciences, Université catholique del Louvain, Chemin du Cyclotron 2, 1348 Louvain-la-Neuve, Belgium
[9] Istituto di Astrofisica e Planetologia Spaziali, IAPS-INAF, Via del Fosso del Cavaliere 100, 00133 Rome, Italy
[10] Instituto de Astrofisica de Andalucia, IAA-CSIC, Glorieta de la Astronomia, 18008 Granada, Spain
[11] School of Physical Sciences, The Open University, Milton Keynes, MK7 6AA, UK
[12] Space Science and Technology Department, Science and Technology Facilities Council, Rutherford Appleton Laboratory, Oxfordshire, U.K.

*Corresponding author: Giuliano Liuzzi (giuliano.liuzzi@nasa.gov)

Key Points:

- Cl isotopic ratio in atmospheric HCl on Mars is measured with NOMAD, finding a slight depletion of ^{37}Cl compared to Earth Standard.
- The atmospheric Cl isotopic ratio is compatible with surface values measured by MSL, not showing any fractionation beyond uncertainties.
- The majority of possible HCl depletion processes at Mars yield residual HCl with lighter Cl than its source.

Abstract

Following the recent detection of HCl in the atmosphere of Mars by ExoMars/Trace Gas Orbiter, we present here the first measurement of the $^{37}Cl/^{35}Cl$ isotopic ratio in the Martian atmosphere using a set of NOMAD observations. We determine an isotopic anomaly of -6 ±78‰ compared to Earth standard, consistent with the -51‰ to -1‰ measured on Mars' surface by Curiosity. The measured isotopic ratio is also consistent with surface measurements, and suggests that Cl reservoirs may have undergone limited processing since formation in the Solar Nebula. The examination of possible sources and sinks of HCl shows only limited pathways to short-term efficient Cl fractionation and many plausible reservoirs of "light" Cl.

1 Introduction

Halogens are among the fundamental components of protostellar clouds, and it is commonly accepted that their main reservoirs in the early Solar System are hydrogen halides (i.e. HF, HCl, HBr), as suggested in Dalgarno et al., (1974) and Jura (1974), given their chemical tendency to form these compounds. For this reason, and for its ubiquitous presence, the detection and study of the abundance and properties of HCl on various bodies of the Solar System is crucial to gain a thorough understanding of their evolution in planetary systems.

Chlorine has two stable isotopes, ^{35}Cl and ^{37}Cl, and as with other molecules, the isotopic quantification of chlorine in HCl is recognized as an important metric for characterizing the chemical processes and outgassing history of a planet. Moreover, this was one of the first isotopic systems to be investigated by theoretical studies (Urey & Greiff, 1935). Across the Solar System, the measurement of Cl isotopic composition in solid surface minerals is directly connected to their current chemical composition and how this evolved from the initial reservoirs (e.g. Catling et al. (2010); Eggenkamp et al. (1995)). In this context, volatilization and redox reactions can efficiently induce long-term Cl fractionation, where molecules and complexes with oxidized Cl (Cl^{n+}, n=1,3,5,7) will concentrate ^{37}Cl relative to chlorides (Cl^-). The variations induced by these processes are measured as deviations from the average Cl isotopic ratio found on Earth (Standard Mean Ocean Chlorine, or SMOC: $(^{37}Cl/^{35}Cl)_{SMOC}$=0.31977, e.g. de Groot (2009)), in units of parts per mil (‰): $\delta^{37}Cl = ((^{37}Cl/^{35}Cl)/(^{37}Cl/^{35}Cl)_{SMOC} - 1)\times 1000$, and can be as significant as tens of ‰.

The value of the isotopic $\delta^{37}Cl$ anomaly has been measured across the Solar System and in other regions of stellar and planetary formation (e.g. de Groot, 2009); values are summarized in Figure 1. Generally, variability of the $^{37}Cl/^{35}Cl$ ratio is due to the conditions where nucleosynthesis of the observed Cl takes place, which is produced almost entirely in core-collapse supernovae. Higher metallicity core-collapse supernovae tend to produce higher $^{37}Cl/^{35}Cl$ ratios (Kobayashi et al., 2006). In the Solar System, the average measured ratios fluctuate between 0.29 and 0.33, while in neighboring star formation regions the measured value can be significantly different. At formation, several mechanisms (primarily degassing and oxidation) are able to increase the $^{37}Cl/^{35}Cl$ ratio of planetary materials, while those that deplete the heavier isotope are usually less efficient (Gargano & Sharp, 2019); therefore, the composition of Cl may be a reliable metric to quantify how much a celestial body has evolved from the original protosolar nebula composition (Dhooghe et al., 2017).

As seen in Figure 1, the Solar System is characterized by a few notable exceptions to SMOC. Mass spectrometric measurements of lunar rock samples (Boyce et al., 2015; Shearer et al., 2014) have shown that the Moon contains chlorine that is isotopically unlike any other body in the Solar System (J. J. Barnes et al., 2019; Sharp et al., 2010). This anomaly has been recently suggested to be the result of degassing of the lunar magma ocean early in the Moon's history, rather than of lava degassing, as initially thought. In a number of cases, instead, the surface δ^{37}Cl is found to be significantly lower than SMOC. Besides Mars' perchlorates, observations of δ^{37}Cl at comet 67P by Rosetta/ROSINA (Dhooghe et al., 2017) indicate δ^{37}Cl=-93‰, consistent with the value in the protosolar nebula (Anders & Grevesse, 1989; Kama et al., 2015; Lodders, 2010). On Earth, the only large exception to the SMOC are the Atacama Desert perchlorates (Böhlke et al., 2005), whose composition is likely due to atmospheric photochemical reactions and subsequent dry deposition onto an arid environment.

The role of atmosphere-surface interactions in determining the variation and present values of δ^{37}Cl on Mars is an outstanding scientific question, which can only be solved by atmospheric measurements supporting existing modeling efforts. While on Earth these dynamics are well studied (e.g. Keppler et al. (2020); Laube et al. (2010)) there is no definite explanation of the peculiarly "light" Cl isotopic composition found at Mars' surface. The widespread observation of perchlorates by the Phoenix lander (Hecht et al., 2009) and by the Sample Analysis at Mars (Mahaffy et al., 2012) onboard Curiosity rover (Glavin et al., 2013) suggested mechanisms similar to those in place for the Atacama perchlorates. Those arid-environment perchlorates are produced by oxidation of Cl species by ozone, or oxygen-containing species (e.g., O or OH) derived from chemical processes involving ozone (Catling et al., 2010), with little or no subsequent evolution. Yet, it was later found that these mechanisms cannot explain - under Martian conditions - the perchlorate abundance measured on Mars (Smith et al., 2014).

The systematically negative values of δ^{37}Cl measured on surface by Curiosity in various locations of Gale Crater (Farley et al., 2016) have at least two plausible explanations related to the thermal evolution of Cl: First, if the measured Cl derived directly from oxychlorine compounds, then the "light" Cl comes from long-term atmospheric chemical transformations involving oxygen compounds. Second, if Cl comes from chloride, partial reduction of isotopically "heavy" perchlorate can fractionate HCl yielding lower δ^{37}Cl (Farley et al., 2016). Because of the depletion in ^{37}Cl, it seems logical to exclude that the origin of the low surface δ^{37}Cl observed is outgassing and subsequent atmospheric escape, which would yield an enrichment in the heavier isotope (Jakosky et al., 2017).

Recently, the Trace Gas Orbiter Atmospheric Chemistry Suite (ACS) and the Nadir Occultation for MArs Discovery (NOMAD) spectrometers reported the first detection of HCl in the Martian atmosphere (Korablev et al., 2021; Aoki et al., 2021). In Martian Year (MY) 34, HCl has been detected by NOMAD in about 50 vertical profiles at L_S = 210-330 right after the most intense phase of the Global Dust Storm (GDS), when the dust content in the atmosphere was still heavily enhanced (Smith, 2004; Smith et al., 2013). Observations show that the enhancement of the HCl abundance in the atmosphere is only transient, in fact previous studies were able to set only upper limits for HCl (e.g. Villanueva et al., 2013) using ground based observations that were acquired around the Northern Spring Equinox (L_S 0), after the period where HCl is reported

by ACS and NOMAD. The detection of HCl therefore constitutes the proof of active exchange of Cl between the surface and the atmosphere in specific conditions.

Here we show the measurement of the $^{37}Cl/^{35}Cl$ isotopic ratio in the atmosphere of Mars obtained with NOMAD, and discuss the implications of this result. To date, this is only the third case in which a value is obtained for a planetary atmosphere (besides Earth and Venus (Iwagami et al., 2008)). The purpose of the present work is two-fold: first, the measured isotopic ratio will be discussed in light of the processes that explain the transient presence of HCl in the Martian atmosphere, discussed in Aoki et al. (2021), Korablev et al. (2021) and Olsen et al. (2021). Second, the significance of the retrieved isotopic ratio is contextualized in connection with the surface value, offering some clues about the atmosphere-surface interaction, and compared to the other values measured in the Solar System.

2 Measurement of $\delta^{37}Cl$ in HCl with NOMAD onboard Trace Gas Orbiter

The ExoMars Trace Gas Orbiter (Vandaele et al., 2018) NOMAD spectrometer operates in the spectral ranges between 0.2 and 4.3 μm. The two infrared channels of NOMAD, one dedicated to Solar Occultations (SO) and one primarily to Limb and Nadir Observations (LNO) combine the optical setup of an echelle grating with an Acousto Optical Tunable Filter (AOTF), which is a feasible way to select diffraction orders during repeated acquisitions (Neefs et al., 2015). During a Solar Occultation measurement, the instrument observes solar radiation as it is attenuated by the atmosphere at different altitudes, switching between five or six diffraction orders every second, providing information about the vertical structure of the atmosphere at a high vertical sampling (~1 km) and spatial resolution (~2 km) from the surface to 200 km. The resolving power of the SO channel is close to 20,000 and obtains vertical profiles of the atmospheric constituents (Vandaele et al., 2015), such as CO_2, H_2O, CO and their isotopologues (Aoki et al., 2019; Vandaele et al., 2019; Villanueva et al., 2021). Pertinent to this work, it also performs a sensitive search of organic species (Korablev et al., 2019), such as hydrocarbons (CH_4, C_2H_4, C_2H_6, Knutsen et al. 2021), and other trace species (e.g. NH_3, N_2O, HCN, OCS, SO_2).

Following the first detection of HCl in the Martian atmosphere reported by ACS (Korablev et al., 2021) and NOMAD (Aoki et al., 2021), we derive the $^{37}Cl/^{35}Cl$ isotopic ratio on a set of occultations where high HCl abundance has been detected, increasing the likelihood of obtaining a statistically significant Cl isotopic ratio estimate. Specifically, we have selected all the detections of HCl during MY34 using the NOMAD spectra that cover the interval 2898 – 2921 cm^{-1} (order 129), which display the R0 lines for the two Cl isotopes (2904.11 and 2906.25 cm^{-1}). Among the ~50 detections of MY34, a number of occultations at mid to high southern latitude (30-75^o S) show the largest HCl abundance, up to 4 ppbv below 40 km. To maximize the signal to noise ratio (SNR) of both the $H^{35}Cl$ and $H^{37}Cl$ lines, we focus on those observations, and select a total of 7 independent occultations where HCl is detected between 2 and 40 km of altitude, at L_S = 250 to 320 in MY34. It is important to point out that in most cases the $H^{37}Cl$ line has intensity below or comparable to the single-spectrum noise level; therefore, a vertical profile of $^{37}Cl/^{35}Cl$ cannot be consistently retrieved. Instead, the data are used to derive an average, global value of $\delta^{37}Cl$ in two steps: first, single spectra are analyzed to derive the $H^{35}Cl$ abundance by only probing the lines of the main isotopologue. Second, we build an average of all those spectra where HCl is detected, weighing them with the SNR of the $H^{35}Cl$ detection, and

retrieve a single value for the $^{37}Cl/^{35}Cl$ isotopic ratio from this "grand average" spectrum. All the analysis is done taking into account the known instrument systematics, such as temperature-induced frequency shifts and resolving power variability, which are modeled and accounted for, according to the instrument calibration (Liuzzi et al., 2019).

Retrievals are performed with the Planetary Spectrum Generator (PSG, Villanueva et al., (2018)) which incorporates an Optimal Estimation retrieval scheme (Liuzzi et al., 2016; Rodgers, 2000) and models the above mentioned instrument systematics (details in Supplementary Materials). Besides HCl, we retrieve the vertical profiles of H_2O and HDO, which have distinct absorption lines in the spectral interval considered herein. The other variables, including atmospheric pressure and temperature, are assumed a-priori from the GEM-Mars model (Neary & Daerden, 2018), using a modeled scenario for the MY34 GDS (Liuzzi et al., 2020; Neary et al., 2020).

The derived isotopic ratio, average spectrum, and retrieved HCl profiles are shown in Figure 2. The average of $\delta^{37}Cl$ (relative to SMOC) from all of the measurements taken at altitudes between 2 and 40 km (a total of 351 spectra), where both isotopes are detectable, is -6 ± 78 ‰ ($^{37}Cl/^{35}Cl$ = 0.3179 ± 0.0192). The uncertainty on this value is directly produced by Optimal Estimation and reflects the equivalent radiometric noise on the grand average of the spectra considered. However, the reported confidence interval is also as large as most variations induced by eventual instrumental and temperature profile systematics (details in the Supplementary Materials). The limited precision of the measurement is essentially set by the level of accuracy of the retrieval of $H^{37}Cl$ isotope, which is close to 13-sigma, in contrast to the $H^{35}Cl$, whose precision is around 20-sigma. It is important to stress again that this value refers to specific environmental conditions: all the spectra used in this study are acquired at latitudes between 30-72 ^{o}S, sparse longitudes and L_S 250-320 in MY34.

The confidence interval of the retrieved value encompasses all the values measured at the surface by Curiosity (Farley et al., 2016), and shows in average only a slight depletion in ^{37}Cl compared to SMOC. There are no measurements at the surface at the same latitudes where this dataset is acquired, therefore a direct comparison is not technically possible. This isotopic ratio is an average over a relatively large range of pressures, preventing from ruling out stronger fractionation at higher altitudes or to resolve its vertical behavior.

3 Discussion: atmospheric chemistry and reservoirs

Despite the relative uncertainty in the derived atmospheric $\delta^{37}Cl$, we can contextualize it with respect to hypotheses formulated to explain the transient atmospheric HCl enhancement, the chemical and physical relation with isotopic ratios at surface, and what conclusions can be drawn about the historical evolution of Mars. First, the observed atmospheric fractionation does not suggest significant Cl escape. Already evident from Curiosity measurements, this agrees with the confidence interval for the atmospheric $\delta^{37}Cl$, which is well below the fractionation observed for gases of similar molar mass, such as Ar, a strong indicator of atmospheric loss through solar wind sputtering (Jakosky et al., 2017). Even if HCl enhancement in the atmosphere is only transient, the retrieved value of $\delta^{37}Cl$ is compatible with the hypotheses that crustal Cl reservoirs that contribute to form HCl in the atmosphere have gone through limited or no degassing, otherwise the average atmospheric (and surface) $\delta^{37}Cl$ would have been much higher (as for the

Moon). The fact that HCl is quickly removed from the atmosphere after L_S 330 indicates that the physical or chemical processes that create and sequester HCl from the atmosphere must be dominant over its escape, not surprising given the chemical reactivity of Cl compounds. On long temporal scales (~Myr), redox reactions involving Cl can yield measurable $^{37}Cl/^{35}Cl$ fractionation, particularly if Cl is reduced from perchlorate salts (e.g. Ader et al., 2008).

As observed by Aoki et al. (2021), the vertical distribution of HCl is very similar to water vapor, and in MY34 is observed between the GDS and the regional storm mostly at mid-latitudes in the Southern hemisphere, where both water vapor and dust are abundant during the declining phase of the GDS (Aoki et al., 2019; Liuzzi et al., 2020). The HCl abundances observed during the same season in MY35 are comparable to MY34, suggesting that the simultaneous presence of dust and water vapor – rather than the abundance of dust itself – is key to HCl production. There are two main channels to produce atmospheric HCl: either directly from Cl^- stored in the form of chloride salts (e.g. NaCl, KCl) in lifted dust particles by reaction with HO_2, or by release from the reaction between oxyanions such as perchlorate salts (ClO_4^-) and OH, whose presence is expected from the odd hydrogen cycle of water vapor.

In the first case, atmospheric HCl is produced when Cl is released by dust. Cl release may happen either by direct UV irradiation of dust particles lifted in the atmosphere during the GDS, or as recently suggested (Wang et al., 2020) by electrostatic discharge of dust particles containing chlorides during very intense dust activity. This last mechanism may account to some of the HCl observed in MY34, and be less relevant in MY35 (Aoki et al., 2021). Regardless, the released Cl would subsequently react with HO_2, H_2O_2 and H_2: $H_2O_2 + Cl \rightarrow HCl + HO_2$; $HO_2 + Cl \rightarrow HCl + O_2$ (Lefèvre & Krasnopolsky, 2017) and $H_2 + Cl \rightarrow HCl + H$. In Martian conditions (Smith et al., 2014), the reaction rate with HO_2 is 10^{-3}-$3{\cdot}10^{-3}$ s^{-1} between 0 and 40 km and the one with H_2 is $4{\cdot}10^{-5}$-$2{\cdot}10^{-3}$ s^{-1}, 2 orders of magnitude larger than the H_2O_2 channel ($4{\cdot}10^{-6}$-10^{-4} s^{-1}). Regardless, these mechanisms would not alter the isotopic composition of Cl in HCl with respect to the one in the dust because Cl does not change its oxidation state.

In the second case, HCl production would occur by a reduction mechanism, which can change the oxidation state of Cl in Cl oxyanions (ClO_x^-) to HCl, and induce formation of HCl with an isotopic composition lighter than the surface perchlorates. However, the lifetime of HCl (90 Sols below 15 km, see Aoki et al. (2021)) would be inconsistent with the timescale of fractionation processes due to redox reactions. Importantly, the modeling of Cl Rayleigh distillation (Farley et al., 2016; Schauble et al., 2003) suggests that a reduction >30% of the perchlorates in dust, with a fractionation factor of 0.95, is able to lower the $\delta^{37}Cl$ by 50‰ in the produced HCl over the geologic history of the crust. Yet, a depletion of tens per ‰ of ^{37}Cl in atmospheric HCl is within the confidence interval of our retrievals and therefore does not conclusively exclude this interpretation for long-term fractionation.

On Earth, O_3 plays an important role in the atmospheric Cl chemistry, as seen in Atacama. However, O_3 at Mars is reportedly absent at L_S 250-320 at latitudes where HCl is most abundant (Perrier et al., 2006; Clancy et al., 2016; Willame et al., 2017), thus the presence of other sources of perchlorates beyond those in the lifted dust is unlikely. Because of oxidation, such sources would be enriched in ^{37}Cl, varying the isotopic composition of Cl in HCl significantly.

NOMAD and ACS data suggest that HCl is abundant below the hygropause. As shown in Figure 3, there are at least four mechanisms that, in principle, could efficiently deplete HCl in the middle atmosphere, and each yields a different isotopic signature in the observed HCl compatible with the confidence interval we retrieved for $\delta^{37}Cl$:

1) Given the high abundance of water vapor where HCl is detected (Aoki et al., 2021), a first chemical pathway to destroy HCl could be the reaction with OH: $OH + HCl \rightarrow Cl + H_2O$. This is the major sink for HCl in the stratosphere at Earth (Michelsen et al., 1996), and preserving the oxidation state of Cl, it would not modify its isotopic composition in the residual HCl. Yet, this process is much slower than the production process involving OH (Aoki et al., 2021);

2) HCl could be adsorbed by deposition on ice particles and condensed. Based on what is expected from fractionation of other elements (e.g. H, O), this would deplete ^{37}Cl of HCl, but only above the altitudes at which HCl is detected in this study and to a limited extent (1-2‰, as in Luo et al., 2012). As mentioned, the vertical distributions of HCl and H_2O are very similar, therefore HCl is expected to be trapped in growing water ice particles (Kippenberger et al., 2019). While no water ice has been detected simultaneously with HCl observations, it has a diurnal cycle, and the frequency of water ice clouds following the regional dust storm at L_S 320 increases at mid-southern latitudes (Liuzzi et al., 2020), and could play a role in HCl depletion;

3) Similarly to what happens on Earth with Polar Stratospheric Clouds, there may be heterogeneous chemistry on water ice by reaction with $ClONO_2$, N_2O_5, HOCl (Solomon, 1999). In this case, HCl could be oxidized in Cl_2 or $ClNO_2$. At isotopic equilibrium, the oxidation of Cl would further deplete ^{37}Cl from HCl, to an extent that depends on temperature and abundance of the reagents. However, even if such processes favor the production of OClO and ultimately perchlorates and their deposition on the surface (Wilson et al., 2016), it is expected that heterogeneous chemistry involving water ice is too slow to be considered an efficient sink of HCl and ^{37}Cl, and to dominate over the other processes. Alternatively, Cl_2 and $ClNO_2$ would be destroyed on timescale of a few tens of minutes; Cl would then be produced, which would in turn react quickly with HO_2 to produce HCl (which means that Cl would be reduced to HCl, as before).

4) Differential photolysis could increase the $\delta^{37}Cl$ in atmospheric HCl. On Earth, this effect is as large as 8‰ in CF_2Cl_2 (e.g. Laube et al., 2010). UV radiation of wavelength ~185 nm can even reach Mars' surface, and this process has its maximum efficiency between 5 and 25 km of altitude in Martian conditions, with $H^{35}Cl$ photolysis rate being around 10 cm^{-3} s^{-1}, rivaling with the efficiency of the OH+HCl reaction. This process would yield "heavier" HCl on timescales typical of photolysis (weeks), yet photolysis alone is not able to explain HCl depletion, because it happens on timescales much longer than production by HO_2 (Catling et al., 2010; Heays et al., 2017).

Overall, this set of NOMAD observations of $\delta^{37}Cl$ is in agreement with the surface values, and the majority of plausible depletion processes yield lighter residual HCl. The isotopic composition of HCl, even with the large uncertainty involved in the data, is mostly consistent with the hypothesis that HCl is produced through Cl directly released from lifted dust particles during the GDS (by UV irradiation or electrostatic discharge). Efficient fractionation with respect to the source can occur only via reduction of oxyanions/perchlorates by hydroxyl

radicals, but is unlikely to be significant on the short timescales in which HCl is observed. If the atmospheric isotopic composition is mostly consistent with surface minerals, the atmospheric value can be considered significant to characterize Cl reservoirs where no surface measurement is available. We find no univoque indication of ^{37}Cl enrichment, consistent with the possibility that Cl reservoirs have undergone little processing after planetary formation.

Despite the global circulation of dust during the GDS, potential reservoirs co-located with detections would include southern highland location, a soil bearing negative δ^{37}Cl, and seasonality. Of the 7 detections shown here 6 occur at high latitude (60–72.5°S), where thermodynamics suggests that Ca-perchlorate brine are metastable at surface (Rivera-Valentin et al., 2020). There, a simple cycle may exist, in which Cl precipitates to perchlorate ClO_4^- (Catling et al., 2010). Once at surface, it can either deliquesce and evaporate, releasing Cl (Rivera-Valentin et al., 2020), or be lifted by dust devils, frequent in this season (Balme et al., 2003), where Cl recombines to HCl following one of the reactions mentioned earlier. However, perchlorate may instead percolate downward to the top of the cryosphere, where it can melt and transforms to a shallow brine nappe (e.g., Clifford et al., 2010). Furthermore a site located at 30°S is too close to the Equator for perchlorate brine metastability. If generated there, Cl may rise up from a deep reservoir to the surface using tectonic paths, as suggested by magmatic dykes propagation and extensional fracturing from the Tharsis region during the Hesperian (Mège and Masson, 1996). Moreover, 3 of the 6 high-latitude detections are also associated with deep-rooted crustal fracturing, following another Tharsis-related fracture swarm, and in one case polygonal ground fractures also show resurfacing. Several Cl detections reported by Aoki et al. (2021) also coincide with Tharsis grabens in the northern hemisphere. Overall, the Cl cycle on Mars may involve other reservoirs across the planet in the crust, at the surface, and in the atmosphere. Crustal reservoirs may supply chlorine with δ^{37}Cl down to ~ -5 ‰, which processed may decrease to even lower values.

The strong link between the atmospheric δ^{37}Cl and Cl reservoirs may indicate that Mars has moved from a primordial reducing environment to its current oxidizing one, as suggested by previous studies (Farley et al., 2016; Smith et al., 2014). The atmospheric measurement presented here is lower than most of the inner Solar System, though compatible with both Venus and Earth's values. Further studies to discern the vertical structure and to map the δ^{37}Cl in HCl will be key to assessing the relation between the atmospheric Cl isotopic composition and that at surface and subsurface, and to address whether or not significant fractionation occurs with altitude.

Acknowledgments and Data

ExoMars is a space mission of the European Space Agency (ESA) and Roscosmos. The NOMAD experiment is led by the Royal Belgian Institute for Space Aeronomy (IASB-BIRA), assisted by Co-PI teams from Spain (IAA-CSIC), Italy (INAF-IAPS), and the United Kingdom (Open University). This project acknowledges funding by the Belgian Science Policy Office (BELSPO), with the financial and contractual coordination by the ESA Prodex Office (PEA 4000103401, 4000121493), by the Spanish MICINN through its Plan Nacional and by European funds under grants PGC2018-101836-B-I00 and ESP2017-87143-R (MINECO/FEDER), as well as by UK Space Agency through grants ST/V002295/1, ST/V005332/1 and ST/S00145X/1 and

Italian Space Agency through grant 2018-2-HH.0. The IAA/CSIC team acknowledges financial support from the State Agency for Research of the Spanish MCIU through the "Center of Excellence Severo Ochoa" award for the Instituto de Astrofísica de Andalucía (SEV-2017-0709), and the CBK PAN team from the EXOMHYDR project, carried out within the TEAM programme of the Foundation for Polish Science co-financed by the European Union under the European Regional Development Fund (TEAM/2016-3/20). This work was supported by NASA's Mars Program Office under WBS 604796, "Participation in the TGO/NOMAD Investigation of Trace Gases on Mars" and by NASA's SEEC initiative under Grant Number NNX17AH81A, "Remote sensing of Planetary Atmospheres in the Solar System and Beyond". U.S. investigators were supported by the National Aeronautics and Space Administration. SV acknowledges support from the Belgian Fonds de la Recherche Scientifique-FNRS under grant numbers 30442502 (ET_HOME) and Belgian Science Policy Office BrainBe MICROBE Projects. SA is "Chargé de Recherches" at the F.R.S. - FNRS. FS acknowledges support from the "Institut National des Sciences de l'Univers" (INSU), the "Centre National de la Recherche Scientifique" (CNRS) and "Centre National d'Etudes Spatiales" (CNES) through the "Programme National de Planétologie". SR thanks BELSPO for the FED-tWIN funding (Prf-2019-077-RT-MOLEXO).

The retrieval package used in this study is the Planetary Spectrum Generator, free and available online at https://psg.gsfc.nasa.gov/helpatm.php#retrieval, at the PSG GitHub site: https://github.com/nasapsg/retrievalOE. The data used in this analysis are available at https://nomad.aeronomie.be/index.php/data.

References

Aoki, S., Daerden, F., Viscardy, S., Thomas, I. R., Erwin, J. T., Robert, S. et al. (2021). Annual appearance of hydrogen chloride on Mars and a striking similarity with the water vapor vertical distribution observed by TGO/NOMAD. *Geophysical Research Letters* (Under review).

Ader, M., Chaudhuri, S., Coates, J. D., & Coleman, M. (2008). Microbial perchlorate reduction: A precise laboratory determination of the chlorine isotope fractionation and its possible biochemical basis. *Earth and Planetary Science Letters*, *269*(3), 605–613. https://doi.org/10.1016/j.epsl.2008.03.023

Anders, E., & Grevesse, N. (1989). Abundances of the elements: Meteoritic and solar. *Geochimica et Cosmochimica Acta*, *53*(1), 197–214. https://doi.org/10.1016/0016-7037(89)90286-X

Aoki, S., Vandaele, A. C., Daerden, F., Villanueva, G. L., Liuzzi, G., Thomas, I. R., et al. (2019). Water Vapor Vertical Profiles on Mars in Dust Storms Observed by TGO/NOMAD. *Journal of Geophysical Research: Planets*, *124*(12), 3482–3497. https://doi.org/10.1029/2019JE006109

Barnes, J. D., & Cisneros, M. (2012). Mineralogical control on the chlorine isotope composition of altered oceanic crust. *Chemical Geology*, *326–327*, 51–60. https://doi.org/10.1016/j.chemgeo.2012.07.022

Barnes, J. J., Franchi, I. A., McCubbin, F. M., & Anand, M. (2019). Multiple reservoirs of volatiles in the Moon revealed by the isotopic composition of chlorine in lunar basalts. *Geochimica et Cosmochimica Acta*, *266*, 144–162. https://doi.org/10.1016/j.gca.2018.12.032

Böhlke, J. K., Sturchio, N. C., Gu, B., Horita, J., Brown, G. M., Jackson, W. A., et al. (2005). Perchlorate Isotope Forensics. *Analytical Chemistry*, *77*(23), 7838–7842. https://doi.org/10.1021/ac051360d

Boyce, J. W., Treiman, A. H., Guan, Y., Ma, C., Eiler, J. M., Gross, J., et al. (2015). The chlorine isotope fingerprint of the lunar magma ocean. *Science Advances*, *1*(8), e1500380. https://doi.org/10.1126/sciadv.1500380

Catling, D. C., Claire, M. W., Zahnle, K. J., Quinn, R. C., Clark, B. C., Hecht, M. H., & Kounaves, S. (2010). Atmospheric origins of perchlorate on Mars and in the Atacama. *Journal of Geophysical Research: Planets*, *115*(E1). https://doi.org/10.1029/2009JE003425

Cernicharo, J., Goicoechea, J. R., Daniel, F., Agúndez, M., Caux, E., de Graauw, T., et al. (2010). The ^{35}Cl/^{37}Cl isotopic ratio in dense molecular clouds: HIFI observations of hydrogen chloride towards W3 A. *Astronomy and Astrophysics*, *518*, L115. https://doi.org/10.1051/0004-6361/201014638

Clancy, R., Wolff, M. J., Lefèvre, F., Cantor, B. A., Malin, M. C., & Smith, M. D. (2016). Daily global mapping of Mars ozone column abundances with MARCI UV band imaging. *Icarus*, *266*, 112–133. https://doi.org/10.1016/j.icarus.2015.11.016

Dalgarno, A., de Jong, T., Oppenheimer, M., & Black, J. H. (1974). Hydrogen Chloride in Dense Interstellar Clouds. *The Astrophysical Journal Letters*, *192*, L37. https://doi.org/10.1086/181584

Dhooghe, F., De Keyser, J., Altwegg, K., Briois, C., Balsiger, H., Berthelier, J.-J., et al. (2017). Halogens as tracers of protosolar nebula material in comet 67P/Churyumov–Gerasimenko. *Monthly Notices of the Royal Astronomical Society*, *472*(2), 1336–1345. https://doi.org/10.1093/mnras/stx1911

Eggenkamp, H. G. M., Kreulen, R., & Koster Van Groos, A. F. (1995). Chlorine stable isotope fractionation in evaporites. *Geochimica et Cosmochimica Acta*, *59*(24), 5169–5175. https://doi.org/10.1016/0016-7037(95)00353-3

Farley, K. A., Martin, P., Archer, P. D., Atreya, S. K., Conrad, P. G., Eigenbrode, J. L., et al. (2016). Light and variable 37Cl/35Cl ratios in rocks from Gale Crater, Mars: Possible signature of perchlorate. *Earth and Planetary Science Letters*, *438*, 14–24. https://doi.org/10.1016/j.epsl.2015.12.013

Gargano, A., & Sharp, Z. (2019). The chlorine isotope composition of iron meteorites: Evidence for the Cl isotope composition of the solar nebula and implications for extensive

devolatilization during planet formation. *Meteoritics & Planetary Science*, *54*(7), 1619–1631. https://doi.org/10.1111/maps.13303

Glavin, D. P., Freissinet, C., Miller, K. E., Eigenbrode, J. L., Brunner, A. E., Buch, A., et al. (2013). Evidence for perchlorates and the origin of chlorinated hydrocarbons detected by SAM at the Rocknest aeolian deposit in Gale Crater. *Journal of Geophysical Research: Planets*, *118*(10), 1955–1973. https://doi.org/10.1002/jgre.20144

Godon, A., Jendrzejewski, N., Castrec-Rouelle, M., Dia, A., Pineau, F., Boulègue, J., & Javoy, M. (2004). Origin and evolution of fluids from mud volcanoes in the Barbados accretionary complex1 1Associate editor: M. Kusakabe. *Geochimica et Cosmochimica Acta*, *68*(9), 2153–2165. https://doi.org/10.1016/j.gca.2003.08.021

de Groot, P. A. (Ed.). (2009). Chapter 9 - Chlorine. In *Handbook of Stable Isotope Analytical Techniques* (pp. 721–722). Amsterdam: Elsevier. https://doi.org/10.1016/B978-0-444-51115-7.00009-7

Heays, A. N., Bosman, A. D., & Dishoeck, E. F. van. (2017). Photodissociation and photoionisation of atoms and molecules of astrophysical interest. *Astronomy & Astrophysics*, *602*, A105. https://doi.org/10.1051/0004-6361/201628742

Hecht, M. H., Kounaves, S. P., Quinn, R. C., West, S. J., Young, S. M. M., Ming, D. W., et al. (2009). Detection of Perchlorate and the Soluble Chemistry of Martian Soil at the Phoenix Lander Site. *Science*, *325*(5936), 64–67. https://doi.org/10.1126/science.1172466

Iwagami, N., Ohtsuki, S., Tokuda, K., Ohira, N., Kasaba, Y., Imamura, T., et al. (2008). Hemispheric distributions of HCl above and below the Venus' clouds by ground-based 1.7μm spectroscopy. *Planetary and Space Science*, *56*(10), 1424–1434. https://doi.org/10.1016/j.pss.2008.05.009

Jakosky, B. M., Slipski, M., Benna, M., Mahaffy, P., Elrod, M., Yelle, R., et al. (2017). Mars' atmospheric history derived from upper-atmosphere measurements of ^{38}Ar/^{36}Ar. *Science*, *355*(6332), 1408–1410. https://doi.org/10.1126/science.aai7721

Jura, M. (1974). Chlorine-Bearing Molecules in Interstellar Clouds. *The Astrophysical Journal Letters*, *190*, L33. https://doi.org/10.1086/181497

Kama, M., Caux, E., López-Sepulcre, A., Wakelam, V., Dominik, C., Ceccarelli, C., et al. (2015). Depletion of chlorine into HCl ice in a protostellar core - The CHESS spectral survey of OMC-2 FIR 4. *Astronomy & Astrophysics*, *574*, A107. https://doi.org/10.1051/0004-6361/201424737

Keppler, F., Barnes, J. D., Horst, A., Bahlmann, E., Luo, J., Nadalig, T., et al. (2020). Chlorine Isotope Fractionation of the Major Chloromethane Degradation Processes in the Environment. *Environmental Science & Technology*, *54*(3), 1634–1645. https://doi.org/10.1021/acs.est.9b06139

Kippenberger, M., Schuster, G., Lelieveld, J., & Crowley, J. N. (2019). Trapping of HCl and oxidised organic trace gases in growing ice at temperatures relevant to cirrus clouds. *Atmospheric Chemistry and Physics*, *19*(18), 11939–11951. https://doi.org/10.5194/acp-19-11939-2019

Knutsen, E. W., Villanueva, G. L., Liuzzi, G., Crismani, M. M. J., Mumma, M. J., Smith, M. D., et al. (2020). Comprehensive investigation of Mars methane and organics with ExoMars/NOMAD. *Icarus*, 114266. https://doi.org/10.1016/j.icarus.2020.114266

Kobayashi, C., Umeda, H., Nomoto, K., Tominaga, N., & Ohkubo, T. (2006). Galactic Chemical Evolution: Carbon through Zinc. *The Astrophysical Journal*, *653*(2), 1145–1171. https://doi.org/10.1086/508914

Korablev, O., Vandaele, A. C., Montmessin, F., Fedorova, A. A., Trokhimovskiy, A., Forget, F., et al. (2019). No detection of methane on Mars from early ExoMars Trace Gas Orbiter observations. *Nature*, 1. https://doi.org/10.1038/s41586-019-1096-4

Korablev, O., Olsen, K. S., Trokhimovskiy, A., Lefèvre, F., Montmessin, F., Fedorova, A. A., et al. (2021). Transient HCl in the atmosphere of Mars. *Science Advances*, *7*(7), eabe4386. https://doi.org/10.1126/sciadv.abe4386

Laube, J. C., Kaiser, J., Sturges, W. T., Bonisch, H., & Engel, A. (2010). Chlorine Isotope Fractionation in the Stratosphere. *Science*, *329*(5996), 1167–1167. https://doi.org/10.1126/science.1191809

Lefèvre, F., & Krasnopolsky, V. (2017). Atmospheric Photochemistry. In F. Forget, M. D. Smith, R. T. Clancy, R. W. Zurek, & R. M. Haberle (Eds.), *The Atmosphere and Climate of Mars* (pp. 405–432). Cambridge: Cambridge University Press. https://doi.org/10.1017/9781139060172.013

Liuzzi, G., Masiello, G., Serio, C., Venafra, S., & Camy-Peyret, C. (2016). Physical inversion of the full IASI spectra: Assessment of atmospheric parameters retrievals, consistency of spectroscopy and forward modelling. *Journal of Quantitative Spectroscopy and Radiative Transfer*, *182*, 128–157. https://doi.org/10.1016/j.jqsrt.2016.05.022

Liuzzi, Giuliano, Villanueva, G. L., Mumma, M. J., Smith, M. D., Daerden, F., Ristic, B., et al. (2019). Methane on Mars: New insights into the sensitivity of CH4 with the NOMAD/ExoMars spectrometer through its first in-flight calibration. *Icarus*, *321*, 671–690. https://doi.org/10.1016/j.icarus.2018.09.021

Liuzzi, Giuliano, Villanueva, G. L., Crismani, M. M. J., Smith, M. D., Mumma, M. J., Daerden, F., et al. (n.d.). Strong variability of Martian water ice clouds during dust storms revealed from ExoMars Trace Gas Orbiter/NOMAD. *Journal of Geophysical Research: Planets*, *n/a*(n/a), e2019JE006250. https://doi.org/10.1029/2019JE006250

Lodders, K. (2010). Solar System Abundances of the Elements. In A. Goswami & B. E. Reddy (Eds.), *Principles and Perspectives in Cosmochemistry* (pp. 379–417). Berlin, Heidelberg: Springer. https://doi.org/10.1007/978-3-642-10352-0_8

Luo, C., Xiao, Y., Ma, H., Ma, Y., Zhang, Y., & He, M. (2012). Stable isotope fractionation of chlorine during evaporation of brine from a saline lake. *Chinese Science Bulletin*, *57*(15), 1833–1843. https://doi.org/10.1007/s11434-012-4994-5

Mahaffy, P. R., Webster, C. R., Cabane, M., Conrad, P. G., Coll, P., Atreya, S. K., et al. (2012). The Sample Analysis at Mars Investigation and Instrument Suite. *Space Science Reviews*, *170*(1–4), 401–478. https://doi.org/10.1007/s11214-012-9879-z

Michelsen, H. A., Salawitch, R. J., Gunson, M. R., Aellig, C., Kämpfer, N., Abbas, M. M., et al. (1996). Stratospheric chlorine partitioning: Constraints from shuttle-borne measurements of [HCl], [ClNO3], and [ClO]. *Geophysical Research Letters*, *23*(17), 2361–2364. https://doi.org/10.1029/96GL00787

Neary, L., & Daerden, F. (2018). The GEM-Mars general circulation model for Mars: Description and evaluation. *Icarus*, *300*, 458–476. https://doi.org/10.1016/j.icarus.2017.09.028

Neary, L., Daerden, F., Aoki, S., Whiteway, J., Clancy, R. T., Smith, M., et al. (n.d.). Explanation for the increase in high altitude water on Mars observed by NOMAD during the 2018 global dust storm. *Geophysical Research Letters*, *0*(ja). https://doi.org/10.1029/2019GL084354

Neefs, E., Vandaele, A. C., Drummond, R., Thomas, I. R., Berkenbosch, S., Clairquin, R., et al. (2015). NOMAD spectrometer on the ExoMars trace gas orbiter mission: part 1—design, manufacturing and testing of the infrared channels. *Applied Optics*, *54*(28), 8494. https://doi.org/10.1364/AO.54.008494

Olsen, K. S., Trokhimovskiy, A., Montabone, L., Fedorova, A. A., Luginin, M., Lefèvre, F., et al. (2021). Seasonal reappearance of HCl in the atmosphere of Mars during the Mars year 35 dusty season. *Astronomy & Astrophysics*. https://doi.org/10.1051/0004-6361/202140329

Perrier, S., Bertaux, J. L., Lefèvre, F., Lebonnois, S., Korablev, O., Fedorova, A., & Montmessin, F. (2006). Global distribution of total ozone on Mars from SPICAM/MEX UV measurements. *Journal of Geophysical Research*, *111*(E9). https://doi.org/10.1029/2006JE002681

Rodgers, C. D. (2000, July 1). Inverse Methods for Atmospheric Sounding | Series on Atmospheric, Oceanic and Planetary Physics. Retrieved June 14, 2019, from https://www.worldscientific.com/worldscibooks/10.1142/3171

Schauble, E. A., Rossman, G. R., & Taylor, H. P. (2003). Theoretical estimates of equilibrium chlorine-isotope fractionations. *Geochimica et Cosmochimica Acta*, *67*(17), 3267–3281. https://doi.org/10.1016/S0016-7037(02)01375-3

Sharp, Z. D., Shearer, C. K., McKeegan, K. D., Barnes, J. D., & Wang, Y. Q. (2010). The Chlorine Isotope Composition of the Moon and Implications for an Anhydrous Mantle. *Science*, *329*(5995), 1050–1053. https://doi.org/10.1126/science.1192606

519 Shearer, C. K., Sharp, Z. D., Burger, P. V., McCubbin, F. M., Provencio, P. P., Brearley, A. J., &
520 Steele, A. (2014). Chlorine distribution and its isotopic composition in "'rusty rock'"
521 66095. Implications for volatile element enrichments of "'rusty rock'" and lunar soils,
522 origin of " 'rusty'" alteration, and volatile element behavior on the Moon. *GEOCHIMICA*
523 *ET COSMOCHIMICA ACTA*, *139*, 411–433.

524 Smith, M. D. (2004). Interannual variability in TES atmospheric observations of Mars during
525 1999–2003. *Icarus*, *167*(1), 148–165. https://doi.org/10.1016/j.icarus.2003.09.010

526 Smith, M. D., Wolff, M. J., Clancy, R. T., Kleinböhl, A., & Murchie, S. L. (2013). Vertical
527 distribution of dust and water ice aerosols from CRISM limb-geometry observations.
528 *Journal of Geophysical Research: Planets*, *118*(2), 321–334.
529 https://doi.org/10.1002/jgre.20047

530 Smith, M. L., Claire, M. W., Catling, D. C., & Zahnle, K. J. (2014). The formation of sulfate,
531 nitrate and perchlorate salts in the martian atmosphere. *Icarus*, *231*, 51–64.
532 https://doi.org/10.1016/j.icarus.2013.11.031

533 Solomon, S. (1999). Stratospheric ozone depletion: A review of concepts and history. *Reviews of*
534 *Geophysics*, *37*(3), 275–316. https://doi.org/10.1029/1999RG900008

535 Urey, H. C., & Greiff, L. J. (1935). Isotopic Exchange Equilibria. *Journal of the American*
536 *Chemical Society*, *57*(2), 321–327. https://doi.org/10.1021/ja01305a026

537 Vandaele, A. C., Lopez-Moreno, J.-J., Patel, M. R., Bellucci, G., Daerden, F., Ristic, B., et al.
538 (2018). NOMAD, an Integrated Suite of Three Spectrometers for the ExoMars Trace Gas
539 Mission: Technical Description, Science Objectives and Expected Performance. *Space*
540 *Science Reviews*, *214*(5). https://doi.org/10.1007/s11214-018-0517-2

541 Vandaele, A.C., Neefs, E., Drummond, R., Thomas, I. R., Daerden, F., Lopez-Moreno, J.-J., et
542 al. (2015). Science objectives and performances of NOMAD, a spectrometer suite for the
543 ExoMars TGO mission. *Planetary and Space Science*, *119*, 233–249.
544 https://doi.org/10.1016/j.pss.2015.10.003

545 Vandaele, Ann Carine, Korablev, O., Daerden, F., Aoki, S., Thomas, I. R., Altieri, F., et al.
546 (2019). Martian dust storm impact on atmospheric H 2 O and D/H observed by ExoMars
547 Trace Gas Orbiter. *Nature*, 1. https://doi.org/10.1038/s41586-019-1097-3

548 Villanueva, G. L., Mumma, M. J., Novak, R. E., Radeva, Y. L., Käufl, H. U., Smette, A., et al.
549 (2013). A sensitive search for organics (CH4, CH3OH, H2CO, C2H6, C2H2, C2H4),
550 hydroperoxyl (HO2), nitrogen compounds (N2O, NH3, HCN) and chlorine species (HCl,
551 CH3Cl) on Mars using ground-based high-resolution infrared spectroscopy. *Icarus*,
552 *223*(1), 11–27. https://doi.org/10.1016/j.icarus.2012.11.013

553 Villanueva, G. L., Smith, M. D., Protopapa, S., Faggi, S., & Mandell, A. M. (2018). Planetary
554 Spectrum Generator: An accurate online radiative transfer suite for atmospheres, comets,
555 small bodies and exoplanets. *Journal of Quantitative Spectroscopy and Radiative*
556 *Transfer*, *217*, 86–104. https://doi.org/10.1016/j.jqsrt.2018.05.023

Wallström, S. H. J., Muller, S., Roueff, E., Le Gal, R., Black, J. H., & Gérin, M. (2019). Chlorine-bearing molecules in molecular absorbers at intermediate redshifts. *Astronomy & Astrophysics*, *629*, A128. https://doi.org/10.1051/0004-6361/201935860

Wang, A., Yan, Y., Jolliff, B. L., McLennan, S. M., Wang, K., Shi, E., & Farrell, W. M. (2020). Chlorine Release From Common Chlorides by Martian Dust Activity. *Journal of Geophysical Research: Planets*, *125*(6), e2019JE006283. https://doi.org/10.1029/2019JE006283

Willame, Y., Vandaele, A. C., Depiesse, C., Lefèvre, F., Letocart, V., Gillotay, D., & Montmessin, F. (2017). Retrieving cloud, dust and ozone abundances in the Martian atmosphere using SPICAM/UV nadir spectra. *Planetary and Space Science*, *142*, 9–25. https://doi.org/10.1016/j.pss.2017.04.011

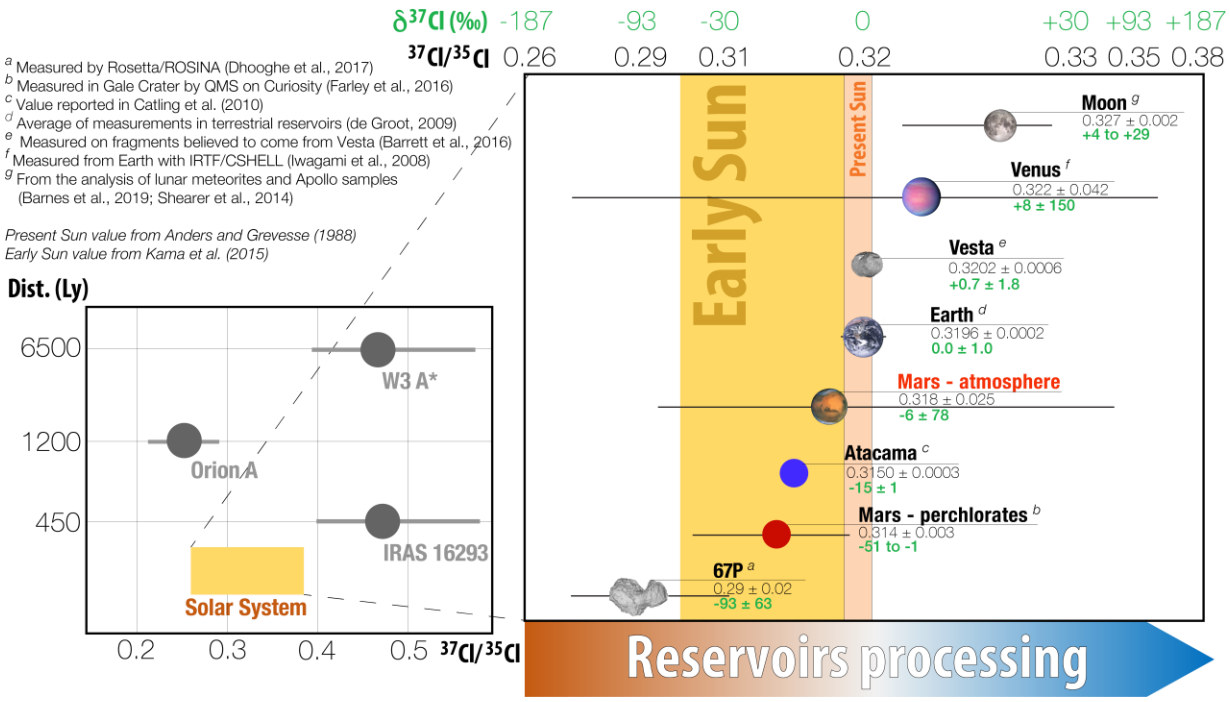

Figure 1. *The isotopic abundances of Cl exhibit a relatively large variability across different regions of our galaxy. Values measured within the Solar System are on the right plot, compared to modeled primordial Sun value. The value from this work is in red text. Values range from the isotopically "heavy" Moon, and the "light" comet 67P. The value measured for Venus and this work are the only cases of infrared spectroscopy measurements, while the others are obtained from mass spectrometry. For the Solar System, values are reported both in terms of absolute ratio, and deviation from SMOC. X-axis is not in linear scale.*

570
571

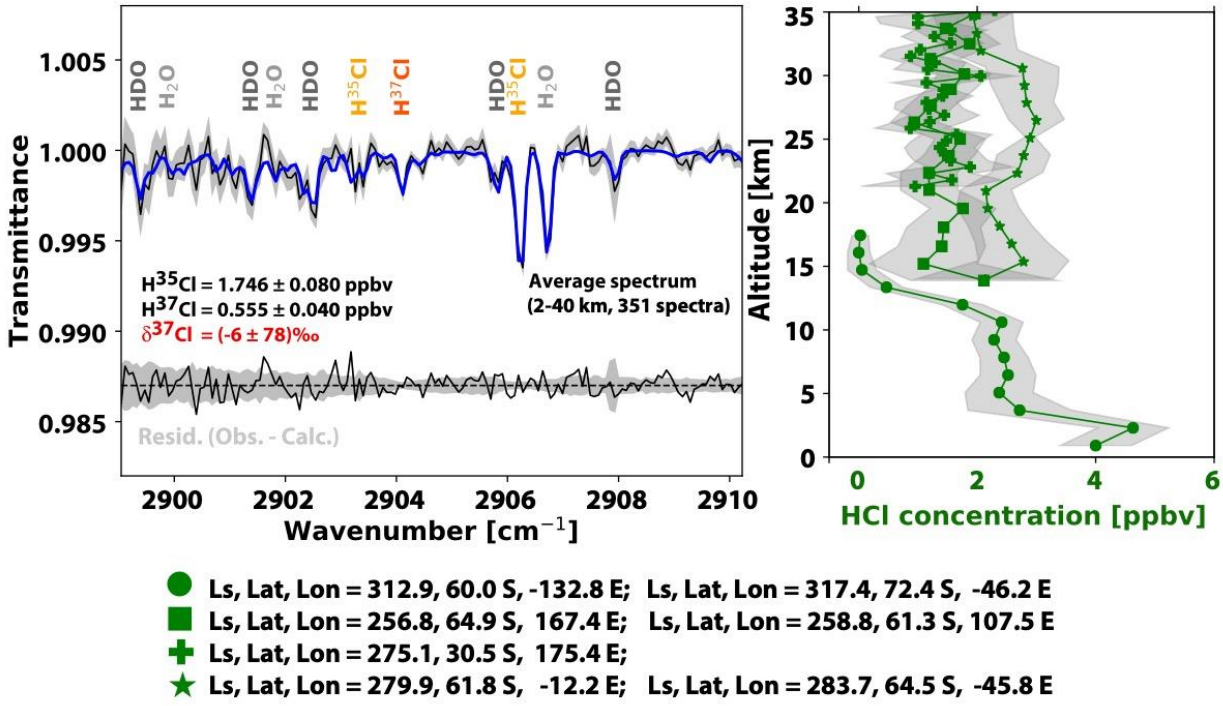

Figure 2. *Average NOMAD spectrum and retrieval of $\delta^{37}Cl$ value. Left panel: observed spectrum (black), best-fit model (blue) and noise (grey). Residuals are on the bottom, and spectral lines are labeled on top. Right panel: vertical profile of of HCl retrieved from the seven occultations considered in this study. Season and location of the occultations are labeled on the bottom. Each profile is an average of two occultations, with the exception of the one at Ls 275-276.*

572
573

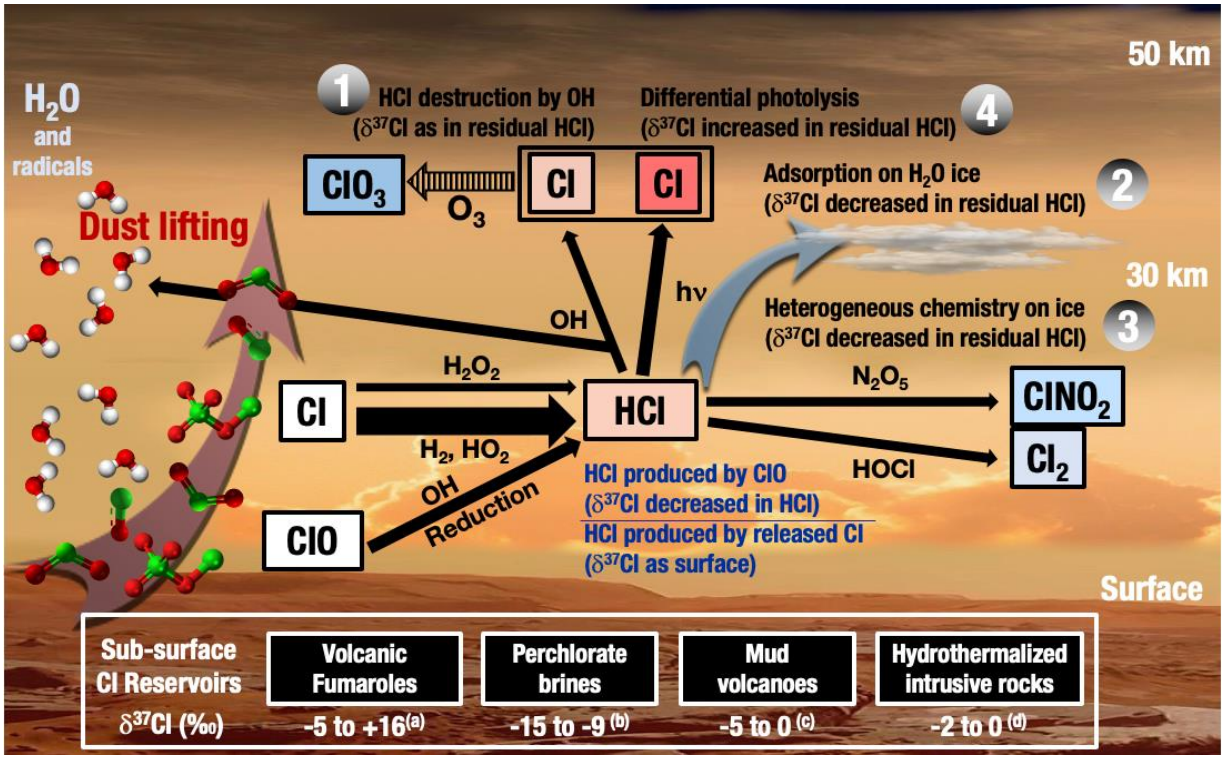

Figure 3. *Proposed HCl physics and chemistry and relation with the Cl isotopic composition and reservoirs. Once produced, HCl is then either deposited after photo- or chemical dissociation or processing through heterogeneous chemistry (involving HOCl, N_2O_5) or adsorption on water ice. The more efficient processes (under Martian conditions) have thicker arrows; the chemistry of O_3 (dashed arrow) is likely not active at the observations' time. Products with the same isotopic composition as the possible surface reservoirs are in white boxes, those that could be depleted in ^{37}Cl compared to sources are in red boxes, and those enriched in ^{37}Cl are in blue. References: (a)Sharp et al. (2010); (b)Böhlke et al. (2005); (c) Godon et al. (2004); (d) Barnes & Cisneros (2012).*

574